

Electrical conductivity of the composite thin films of polyvinylpyrrolidone impregnated with nickel oxide nanoparticles.



Zainab Dakheel Abd Ali ^{1*}, Ahamed A. Ahamed ², Ousama Abdul Azeez Dakhil ³,
Omer El-Amin Ahmed Adam ⁴

¹Ministry of Science and Technology, Baghdad, Iraq;

²polymer Research Unit, College of Science, Al-Mustansiriyah University, Iraq

³Physics Department, College of Science, Al-Mustansiriyah University, Iraq

⁴Chemistry Department, Faculty of Science and Arts in Baljurashi, Al-Baha University, Al-Baha, Saudi Arabia

ARTICLE INFO

Received: 26 / 05 / 2023

Accepted: 19 / 06 / 2023

Available online: 12 / 12 / 2023

DOI:10.37652/juaps.2023.140603.1076

Keywords:

PVP polymer, Nickel oxide nanoparticle, hydrothermal synthesis ,electric conductivity, composite thin film, conductive polymer.

Copyright©Authors, 2022, College of Sciences, University of Anbar. This is an open-access article under the CC BY 4.0 license (<http://creativecommons.org/licenses/by/4.0/>).



ABSTRACT

In this study, we prepared composite thin films of polyvinylpyrrolidone polymer by using 0.02-0.2% weight percent nickel oxide nanoparticles (NiONPs). hydrothermal method utilized to produce NiO NPs. By using XRD and FTIR analysis, the crystal structure was thoroughly examined. Surface morphology was well studied by scanning field emission (SEM) and atomic force microscopy (AFM). The optical properties of the composite thin film of PVP-NiO NPs have been characterized. the charge type of the thin film composite and electric properties determined by Hall effect measurement. XRD analysis reveals that NiO NPs have a cubic phase structure. The main chemical bonds of PVP pure have been determined, where Ni-O bonds appear at 408 cm⁻¹ when NiO NPs are added to the polymer matrix. Composite thin film has a lower energy gap than PVP pure. The hall effect measurement shows Composite thin film is p-type and has 2×10^{-4} Sm at 0.2 % wt of NiO NPs. As a result, a composite thin film of PVP-NiO NPs can be utilized as a semi-conductor in photo sensor and solar cell applications.

1.Introduction

The traditional concept of polymer is insulating materials elimination when polyacetylene polymer discovered in 1970s, and Conductive polymers (CPs) entered a new era. Conductive polymers often possess the -conjugated system with alternate single and double bonds, which gives rise to their intrinsic electrical/electronic, electrochemical, and optical capabilities. The conjugation duration, crystallinity, and intra-chain and inter-chain interactions all have an impact on these physical characteristics. Compared to their counterpart, which is inorganic. CPs have benefits such low density, chemical variety, flexibility, adaptable conductivity, easily controllable form, and morphogenesis [1].

Consequently, they might be used in large-area optoelectronic devices [2], absorption of microwaves materials, different kinds of sensors ,storage of energy engineering, anticorrosive coating, physiological field, etc. The well studied CPs also include polyacetylene, polyaniline, polypyrrole, polythiophene, poly(3,4-ethylenedioxythiophene), and poly(p-phenylene vinylene). [4].

Conductive polymers' conductivity is influenced by the kind, concentration of the dopants , quantity, and doping time of their dopants. Dopants can be divided into large polymeric species and tiny cations/anions depending on their molecular size. Because they are tightly attached to the polymer chain, large dopants can be hard to leach from it. Additionally, they affect the physical characteristics, density, and surface topography of CPs. Small dopants, on the other hand, quickly and easily dedope to produce CPs with low stability. The concentration of the dopant and the doping time have a

*Corresponding author at: Ministry of Science and Technology, Baghdad, Iraq;
ORCID:<https://orcid.org/0009-0006-4734-4304>; Tel:+9640000000000000
E-mail address: zainabdakheel@uomustansiriyah.edu.iq

significant impact on the conductivity of CPs, which increases as the doping level increases[5,6]. The conductivity is enhanced by an increase in dopant concentration. Due to the conductive polymers' organized, dense structure, the dopant ions slowly diffuse into them in the meantime. After a lengthy doping period, perhaps even several hours, the conductivity grew progressively saturated. Additionally, the process of doping and dedoping can be reversed [7,8].

The various types of doping techniques include photodoping, chemical doping, which includes vapor-phase doping and solution doping, non-redox doping, electrochemical doping, and charge-injection doping. Chemical and electrochemical doping are most frequently utilized because they are convenient and inexpensive [9,10].

2. Material and Method

2.1 polyvinylpyrrolidone (PVP) polymer

PVP is an amorphous polymer has chemical structure $(C_6H_9N)_n$ that is non-toxic, flexible, and has a number of intriguing characteristics. It has strong environmental stability, is easily processed, is water soluble and biodegradable, is fairly electrically conductive, and has a wealth of physics in charge transfer mechanisms. known as polyvidone or povidone, is created from the monomer N-vinylpyrrolidone [11].

PVP readily absorbs up to 40% of its weight in water while in its dry form, when it is a thin, flaky powder. Because it quickly forms films in solution and has excellent wetting properties, it functions well as a coating or coating additive. PVP is a nonionic, linear, and amphiphilic polymer. a variety of electrolytes and resins are compatible. Esters, ethers, ketones, and hydrocarbons are insoluble, whereas water and polar solvents are soluble. ineffective for thermoplastics processing Oxygen-permeable, strong, glossy, clear, and films that adhere to a range of substrates Hygroscopic properties of adhesion and cohesion Cross-linkable biologically inert[12].

The only factor limiting the concentration of PVP polymer is viscosity. PVP polymer dissolves in cold water. A number of organic solvents, including alcohols, certain chlorinated compounds like chloroform, and

methylene chloride, are also readily soluble in the PVP K-30 polymer. ethylene and isopropanol esters [14].

PVP polymer films are transparent, glossy, and durable when they haven't been altered or dried out. The visual appearance of films made using different solvent systems, like water, ethanol, chloroform, or ethylene dichloride, is unaffected.

2.2 Nickel Oxide Nano particales properties

Nickel Oxide Nano particales, also known as transition metal oxide, It is a metal-deficient p-type semiconductor with an ambient-temperature band gap of between 3.6 and 4.0 eV.

NiO is a green nano-material exhibition high conductivity, optimal switching speed, , and well-defined and steady redox kinetic. As catalysts, NiO films have been used. A substance made of different n-type semiconductors can be used to make batteries, supercapacitors, electrochemical capacitors, gas sensors, humidity sensors, memory devices, high-energy density devices, antibacterial materials, and more. It is ideal for energy conversion and storage devices and is favored as anode materials due to its high theoretical specific capacitance. In addition to their improved functionality and nonvolatile memory capabilities, NiO NPs also offer appealing optical, electrochemical, and magnetic properties.[15,16]

2.3 Nanostructure NiO synthesized by hydrothermal approach

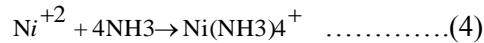
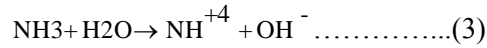
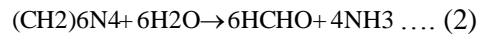
the hydrothermal technique is an intriguing alternative synthetic method. Due to its low treatment temperature and simplicity of controlling particle size, Metal oxide and various other chemicals have been successfully synthesized at the nanoscale using this method. The hydrothermal method enables shaping and sizing of particles by varying reaction temperature, time, and precursor concentration.[17]

for synthesize the nickel oxide nanoparticles, liquids of NiO nitrate as $Ni(NO_3)_2 \cdot 6H_2O$ and hexamethylenetetramine (HMT) ($C_6H_{12}N_4$) was mixed in 80 ml water under stirring [all material purchased from Sigma-Ald].

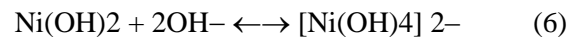
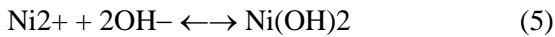
The concentration (weight in grams) of Ni nitrate and (HMT) is dictated by the molarity (M) of the solution, which is 5%, citing [18]

$$M\% = \frac{W}{M.W} * \frac{1000}{V} \dots\dots\dots(1)$$

The chemical reaction to obtain NiO NPs are [15,19]:



Na⁺ is drawn to the OH surrounding the nanocrystal, forming a virtual capping layer that prevents the nanocrystal from developing [20].



Pure crystals of NiO were obtained. One or more of the experimental growth parameters that have a substantial impact on the morphology and aspect ratio are the initial solution pH, precursor concentration, and growth temperature[21].

2.4 Hall Effect measurements

Hall measurements are frequently used to determine whether a semiconductor is n- or p-type and to assess the carrier concentration and mobility during the first characterisation of semiconductors.

Hall Effect's advantage is due to its competence to precisely measure the properties of a specimen of any arbitrary and irregular shape. In practically two dimensions, the sample (with low thickness), and solid (no holes), and "The Van der Pauw Method" [21] has four electrodes with the placement of 1cm around the perimeter of the specimen, and employs a linear four-point probe. In the existence of a z-directional magnetic field (B), a steady current (I) travels along the x-axis from left to right.

at first Electrons are exposed to the Lorentz force ,and They move in the direction of the negative y-axis as a result of a transverse voltage brought on by an excess surface electrical charge on the sample's side. According to Figure, this transverse voltage is referred to as the Hall voltage (V_H).

that forms the Hall field through the specimen thickness (t), as follow[22]:

$$R_H = \frac{V_H}{I} \frac{t}{B} \dots\dots\dots 9$$

We can estimate the carrier's from the Hall coefficient equation. The semiconductor concentration and the carrier type, the sign of R_H if negative or positive which determined n- or p-type, the semiconductor[23]:

$$R_H = \frac{1}{pq} \dots\dots\dots 10. \text{for p-type}$$

$$R_H = \frac{-1}{pq} \dots\dots\dots 11. \text{for n-type}$$

So, (q) is represented electron charge.

$$\sigma_n = q_n \mu_n \dots\dots\dots 12. \text{for n-type}$$

$$\sigma_p = q_p \mu_p \dots\dots\dots 13 \text{ p-type}$$

In the relationship between the Hall coefficient and conductivity (σ), the Hall mobility (μ_H) can also be obtained[24]

$$\mu_H = |R_H| \dots\dots\dots 14$$

Mobility may be calculated by specified (σ) and (R_H).Or can be performed to calculate the films' resistance (ρ)[25]:

$$\rho = R \cdot W \cdot t / L \dots\dots\dots 15$$

W is the electrode's width, L is the distance between the electrodes, and t is the thin film's thickness, where R is the resistance.. The conductivity (σ) of the film based on the relationship , it could be specified [26]:

$$\sigma = 1 / \rho \dots\dots\dots 16$$

2.5 Preparations of Composite thin films

A thin film was formed by casting 1 gm of PVP solvent in 50 ml of water (2% PVP by weight) for 10 minutes at 60 °C. The concentrations of NiO NPs added to the solution were (0.01, 0.02, 0.03, 0.04, 0.05, 0.06, 0.07, 0.08, 0.09, and 0.1 gm). The solutions have to be cast on a glass Petri dish to form a thin film once the solution polymer has dried. According to Fig. 1, a thin film with a thickness of 1 μ is formed over the course of two days using the coating thickness meter CM8829S.



Figure (1): PVP-NiO thin film composite

3.Results and Discussions

3.1 XRD spectrum analysis

Figure 2 shows the PVP-NiO nanopowder that was analyzed using an X-ray diffraction instrument. The results of the NiO NPs data, showed the presence of diffraction peaks at the angles (2θ): 37.20° , 43.20° , 62.87° , 75.20° , and 79.38° , which correspond to the Miller indices (111), (200), (220), (311), and (222), respectively. These Miller indices suggest that the cubic phase of NiO structure is the crystal form of NiO NPs. The diffraction peak data are consistent with the Standard (JCPDS No. 10-0325). Thus, the NiO nanoparticles were cubic structure. The XRD Pattern spectra of NiO NPs matched with [27].

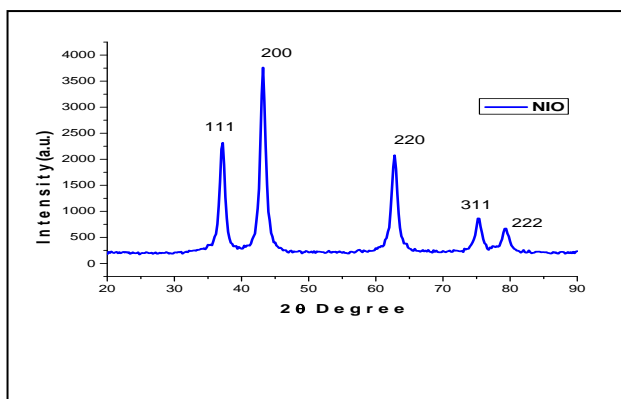


Figure (2) : XRD pattern of NiO NPs

From X-ray diffraction, the mean crystallite size can be calculated using Scherrer's formula, $d = 0.9\lambda / \beta \cos \theta$, where d is the crystallite size, λ is the diffraction wavelength, β is the full width at half maximum, and θ is the X-ray wavelength [28]. The particles' crystalline average size (D) is 25 nm.

3.2 FTIR of PVP-NiO NPS Composite Thin Films

The FTIR spectrum was determined for the pure PVP and composite thin film of PVP-NiO nanostructure, which is displayed in Fig. 3.

The main active groups characteristic of the pure PVP polymer are shown clearly in Figure 3(a) and are as follows: [O-H] stretching, [C-H] asymmetric stretching, and [C=O] stretching vibration. In the FTIR spectrum, C-N stretching, pyrrolidone ring, and CH₂ bending vibration are located at and the two peaks, corresponding wave number at 3434 cm^{-1} , at 2955 cm^{-1} , at 1661 cm^{-1} , 1424 cm^{-1} , 895 cm^{-1} , 1291 , and 1018 respectively. [29,30]

As for PVP doped with NiO NPs 0.2 wt%, there is a difference in the locations of the backbone of PVP active groups due to the interaction with NiO NPs, where a bond Ni-O appears in the 408 cm^{-1} , and this is identical to the research [31] where there was a shift to the right and intensity increased compared with the main active group of PVP pure due to doping processing as shown in figure 3(b)

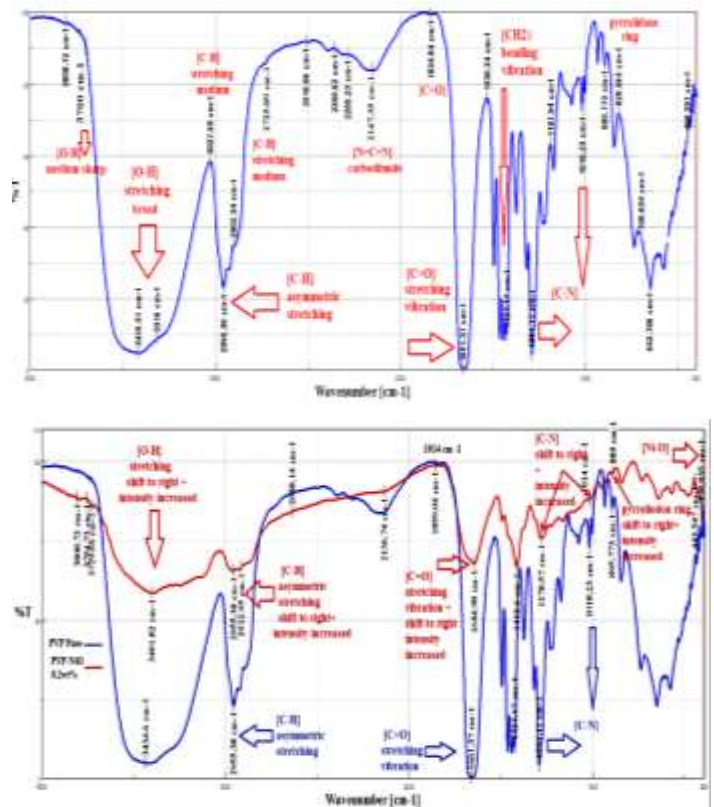


Figure 3(a) shows the curve of the infrared spectrum of a pure PVP in blue line, (b) elucidate overlapping between a PVP

pure (blue line) and PVP- NiO NPs composite thin films (red line) .

3.3 FESEM Images of PVP-NiO nanostructure composite Thin Film

NiO NPs features are depicted Fig. 6 with high-density image of scanning electron microscopic (SEM), synthesized via a hydrothermal approach , Figures 4 (a,b) demonstrate magnification of 1 μ m and 200 nm respectively , that the product is primarily made up of nanoparticles produced with various dimensions of an agglomerated formulation cluster of the nanoparticles. The minimum size of produced nanoparticles is 40.19 nm as shown in Fig 4.(b)

Histogram of The FE-SEM represented in Images (c), according to calculation of Image J software program has been selected 100 particles as a minimum indicates that the particles have a standard deviation of 10.9 nm and an average diameter of 30 nm. NiO particles ranged in size from 11.8 nm at their smallest to 80. nm at their largest.

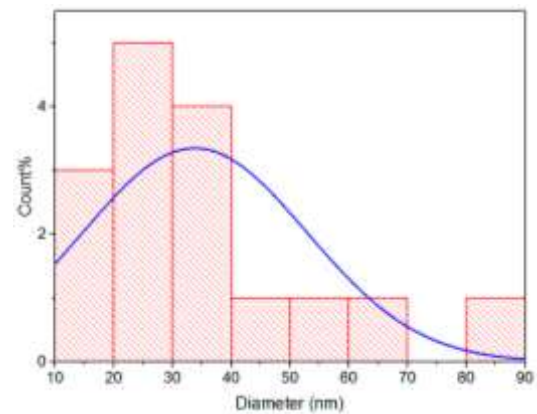


Figure 4. FESEM images of NiO nanoparticles (a) FESEM images of NiO nanoparticles with 1 μ m scale (b) NiO nanoparticles with,200 nm scale exhibit particles size (c) Histogram of The FE-SEM of NiO nanoparticles with size distributions

3.4 AFM

The surface topography and morphology of a PVP-NiO NPs composite thin film were analyzed by atomic force microscopy (AFM) for the sample with nano- and micron-scale dimensions shown in Figure (5) in two dimensions and in three dimensions, respectively

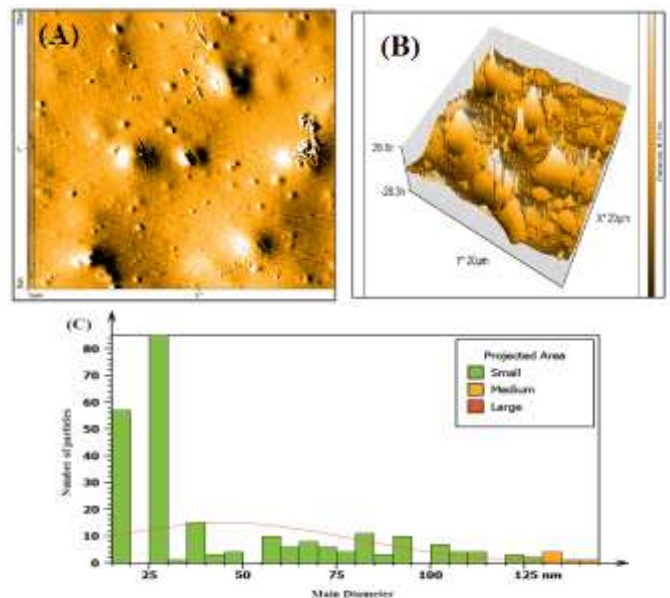
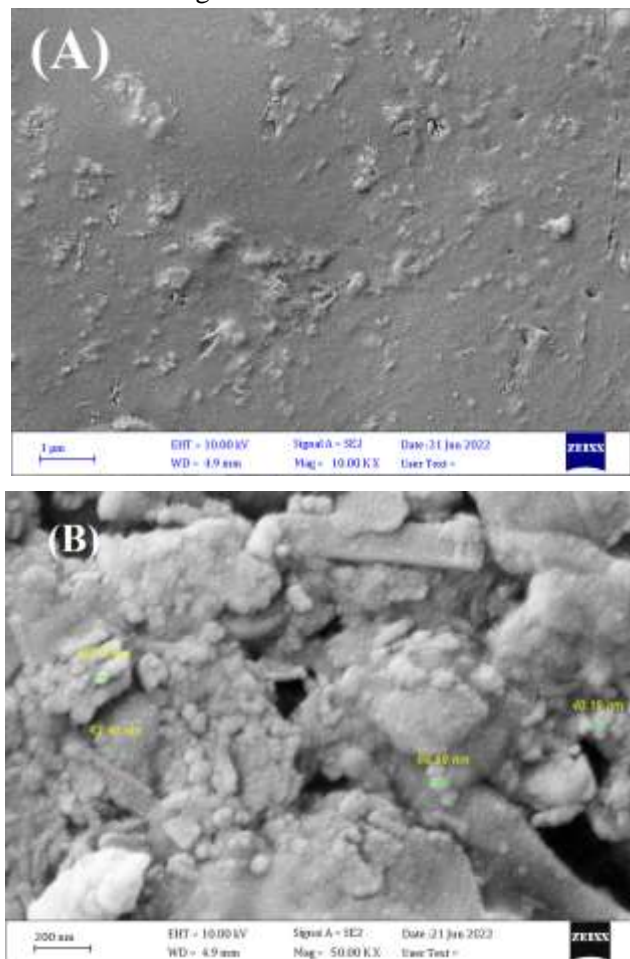


Figure. 5 Section line analysis, (A) topography 2D, and (B)morphology 3D AFM images and (C)particle size distribution of PVP-NiO Composite thin film

It is known that the morphology of the film greatly depends on the formation of nanoporous structures within a thin composite film. The image

shown in Figure (5) indicates that after impregnation of NiO nanoparticles into the composite thin film, the surface becomes much more homogeneous, and the dimensions of most of the particles were smaller than (1.0 μm), which could be due to aggregation of the NiO nanoparticles, which is a very common phenomenon in nanomaterials synthesis. Mean root square height and mean diameter are significant parameters associated with surface roughness with values at the nanoscale, as seen in figure 7 (c), which is consistent with the findings of (SEM IMAGE), which depict particles with nano-scale sizes. This confirms that the casting process is a successful method for the synthesis of a thin film without affecting the nano-size of the NiO particles that are inserted in the PVP matrix.

3.5 Ultraviolet-visible (UV-Vis) spectroscopy analysis

Figure (6) The curve depicted the relation between $(h\nu)$ and $(\alpha h\nu)^2$, where the band gap energy of the thin film is represented by the intercept between the lowest point in the curve and the x-axis, which is (4.8 eV) for PVP pure, and the result coincided with Pan, Mingming, et al.(2020)[20] and Vani, G. Naga Sudha, et al.,2013.[33]

Figure 6 (b) shows that the band gap energy for a thin film of PVP doped with wt%0.2 NO NPs is 4.6 eV smaller than that of PVP pure. This finding is in agreement with Mohammed, M. I., et al. (2022) [34]. band gap of NiO is 3.6 eV while NiO NPs in range (3.6 - 4 eV) [35].

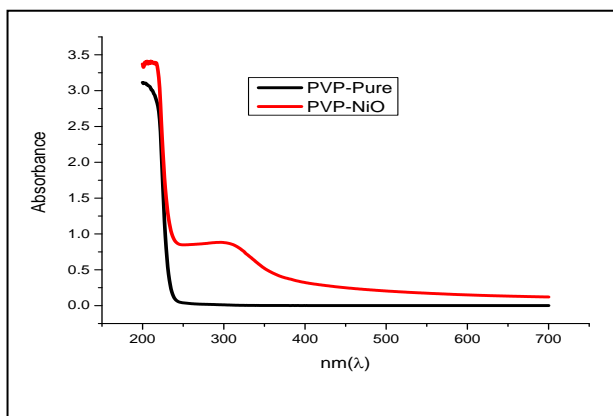


Figure 6(a) UV-Spectra analysis (Absorption spectra versus the wavelength) for PVP Pure thin film (black line) and PVP- NiO Composite thin film (red line) depicted their Absorption versus Of their Wave length.

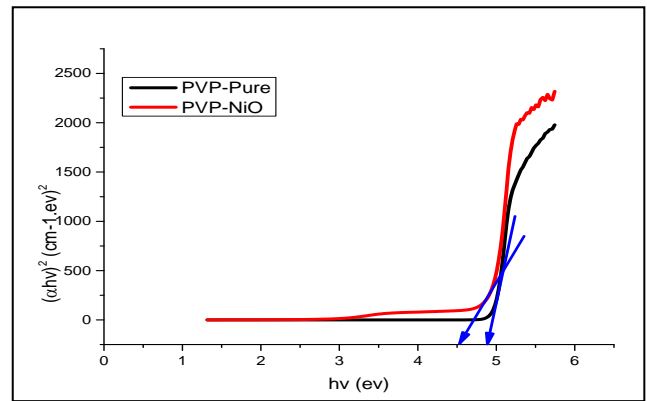


Figure 6 : (b) Energy band gap of PVP Pure thin film (black line) ,(B) Energy band gap of PVP-NiO Composite thin (red line)

3.6 Hall Effect results

In Fig. 9, the thin film's electrical conductivity PVP-NiO NPs composite thin films has been evaluated and plotted as a function of NiO NPs doping concentration at various concentrations in the order of: (0.01, 02, 03, 04, 05, 06, 07.08.09, 0.1) gm, The conductivity increases with concentration, reaching a maximum of (1.091*10⁻⁴) Sm at a concentration of 0.1 gm. Table 1 lists the conductivity, average Hall coefficient, charge type, and mobility of NiO NPs at various concentrations. The P-type doping is in the thin film. The electric conductivity of pure PVP is in the range of 10⁻⁶ and 10⁻⁷ [36].

The doping procedure with NiO NPs increases electrical conductivity by increasing NiO NP concentrations, producing a semiconductor made of PVP-NiO NP composite thin film. The highest value of conductivity was obtained when it was concentrated NiO NPs, which is 0.1 gm.

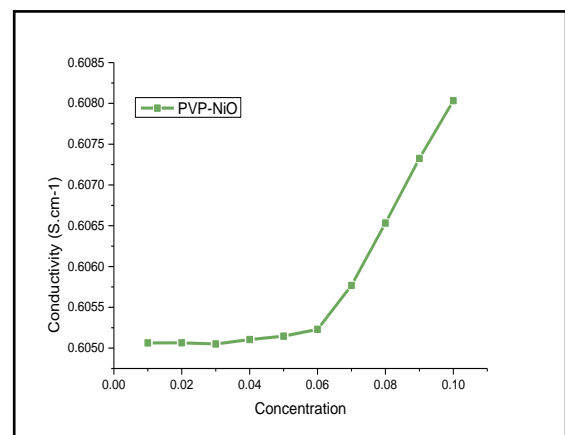


Figure (7). Relationship between conductivity and concentration of PVP- NiO NPs thin film

TABLE .1 measurements of hall effect of PVP-NiO Composite thin films

Concentration (gm)	Conductivity 1/Ω.cm (Sm)	Average Hall Coefficient (m ² /c)	Mobility (cm ² /v.s)
0.01	0.02234*10 ⁻⁵	-1.91434*10+6	1.4731*10 ⁺²
0.02	0.04185*10 ⁻⁵	-1.97033*10+6	1.7457 *10 ⁺²
0.03	0.06153*10 ⁻⁵	-2.01137*10+6	1.8753*10 ⁺²
0.04	0.1431*10 ⁻⁴	-2.10741*10+5	2.073610 ⁺²
0.05	0.1810*10 ⁻⁴	-2.21328*10+5	2.1214*10 ⁺²
0.06	0.2075*10 ⁻⁴	-2.3020*10+5	2.1872*10 ⁺²
0.07	0.4047*10 ⁻⁴	-2.41271*10+5	2.2327*10 ⁺²
0.08	0.6016*10 ⁻⁴	-2.50552*10+5	2.2836*10 ⁺²
0.09	0.827*10 ⁻⁴	-2.60783*10+5	2.3463*10 ⁺²
0.1	0.2080*10 ⁻³	-2.76164*10+4	2.432*10 ⁺²

Conclusion

The hydrothermal method was used to produce nickel oxide nanoparticles, where the scanning electron microscope(SEM) examination image showed the nanoscale size of nickel oxide and the particle size average was calculated and was 30 nanometers, while the X-ray diffraction examination determined the Miller indices, which showed that nickel has a Cubic Phase structure and that the crystalline average size of particles is equal to 25 nanometers, while the atomic force microscope(AFM) image showed the distribution of nanoparticles on the surface of the composite thin film randomly with the appearance of semi-spherical shapes indicating the presence of nickel oxide nanoparticles, we conclude that the polymer was doped with nanoparticles based on the results of the nanoscale size of nickel oxide particles . The energy band gap of a pure polymer is larger compared to With the doped polymer, an increase in the concentration of nickel oxide nanoparticles led to a decrease in the energy gap. The electrical conductivity of the polymer doped with different concentrations increases with increasing concentration, and the best value is at the weight ratio (0.2%). This result shows the effect of adding NiO NPs on both the optical and electrical properties of the polyvinylpyrrolidone polymer.

REFERENCES

1. Kang, Stephen Dongmin, and G. Jeffrey Snyder. "Charge-transport model for conducting polymers." *Nature materials* 16.2 (2017): 252-257 . <https://doi.org/10.1038/nmat4784>

2. Goel, Mahima, et al. "Principles of structural design of conjugated polymers showing excellent charge transport toward thermoelectrics and bioelectronics applications." *Macromolecular Rapid Communications* 40.10 (2019): 1800915. <https://doi.org/10.1002/marc.201800915>
3. Correa, D. S., et al. "Nanostructured conjugated polymers in chemical sensors: synthesis, properties and applications." *Journal of nanoscience and nanotechnology* 14.9 (2014): 6509-6527. <https://doi.org/10.1166/jnn.2014.9362>
4. Balint, Richard, Nigel J. Cassidy, and Sarah H. Cartmell. "Conductive polymers: Towards a smart biomaterial for tissue engineering." *Acta biomaterialia* 10.6 (2014): 2341-2353. <https://doi.org/10.1016/j.actbio.2014.02.015>
5. Chang, Mincheol, et al. "Control of molecular ordering, alignment, and charge transport in solution-processed conjugated polymer thin films." *Polymers* 9.6 (2017): 212. <https://doi.org/10.3390/polym9060212>
6. Jasim, B. E., N. A. A. Aboud, and A. M. Rheima. "Nickel oxide nanofibers manufactured via sol-gel method: synthesis, characterization and use it as a photo-anode in the dye sensitized solar cell." *Digest Journal of Nanomaterials & Biostructures (DJNB)* 17.1 (2022). DOI: [10.15251/DJNB.2022.171.59](https://doi.org/10.15251/DJNB.2022.171.59)
7. Le, Thanh-Hai, Yukyung Kim, and Hyeonseok Yoon. "Electrical and electrochemical properties of conducting polymers." *Polymers* 9.4 (2017): 150. <https://doi.org/10.3390/polym9040150>
8. Jasim, Basma Esam, Zainab Naief Mageed, and Zahraa S. Al-Garawi. "Nanochitosan grafting sodium alginate improve loading and release of the antibiotic 'streptomycin', for drug release applications." *Journal of Physics: Conference Series*. Vol. 1660. No. 1. IOP Publishing, 2020. DOI: [10.1088/1742-6596/1660/1/012030](https://doi.org/10.1088/1742-6596/1660/1/012030)
9. Le, Thanh-Hai, Yukyung Kim, and Hyeonseok Yoon. "Electrical and electrochemical properties of conducting polymers." *Polymers* 9.4 (2017): 150. <https://doi.org/10.3390/polym9040150>
10. Jalal, Noor M., et al. "The effect of sulfonation reaction time on polystyrene electrospun membranes

- as polymer electrolyte." *AIP Conference Proceedings*. Vol. 2290. No. 1. AIP Publishing LLC, 2020. DOI: [10.1038/s41598-022-26270-3](https://doi.org/10.1038/s41598-022-26270-3)
11. Kaewnopparat, Nattha, et al. "Increased solubility, dissolution and physicochemical studies of curcumin-polyvinylpyrrolidone K-30 solid dispersions." *World Academy of Science, Engineering and Technology* 55 (2009): 229-234.pdf
12. Teodorescu, Mirela, and Maria Bercea. "Poly (vinylpyrrolidone)–a versatile polymer for biomedical and beyond medical applications." *Polymer-Plastics Technology and Engineering* 54.9 (2015): 923-943. <https://doi.org/10.1080/03602559.2014.979506>
13. Franco, Paola, and Iolanda De Marco. "The Use of Poly (N-vinyl pyrrolidone) in the Delivery of Drugs: A Review." *Polymers* 12.5 (2020): 1114 DOI: [10.3390/polym13152569](https://doi.org/10.3390/polym13152569)
14. Ingole, Shital A., and Ashok Kumbharkhane. "Temperature dependent Broadband dielectric relaxation study of Aqueous Polyvinylpyrrolidone (PVP K-15, K-30 & K-90) using a TDR." *Physics and Chemistry of Liquids* 59.5 (2021): 806-816. <https://doi.org/10.1080/00319104.2020.1836641>
15. Hong, Sung-Jei, et al. "Characterization of nickel oxide nanoparticles synthesized under low temperature." *Micromachines* 12.10 (2021): 1168. <https://doi.org/10.3390/mi12101168>
16. Jalal, Noor M., Akram R. Jabur, and Shrok Allami. "Effect of Electro-spinning applied Voltage on Electro-spun EPS Membranes Thickness and Fibers Diameters." *Journal of Physics: Conference Series*. Vol. 1879. No. 3. IOP Publishing, 2021. DOI [10.1088/1742-6596/1879/3/032085](https://doi.org/10.1088/1742-6596/1879/3/032085)
17. Xu, Sheng, and Zhong Lin Wang. "One-dimensional ZnO nanostructures: solution growth and functional properties." *Nano research* 4 (2011): 1013-1098 <https://doi.org/10.1007/s12274-011-0160-7>
18. Krishnamurthy, Vijay M., et al. "Dependence of effective molarity on linker length for an intramolecular protein– ligand system." *Journal of the American Chemical Society* 129.5 (2007): 1312-1320 <https://doi.org/10.1021/ja066780e>
- 19 Cao, Shixiu, et al. "Hydrothermal synthesis of nanoparticles-assembled NiO microspheres and their sensing properties." *Physica E: low-dimensional systems and nanostructures* 118 (2020): 113655. <https://doi.org/10.1016/j.physe.2019.113655>
20. Safa, S., et al. "Hydrothermal synthesis of NiO nanostructures for photodegradation of 4-nitrophenol." *Desalination and Water Treatment* 57.46 (2016): 21982-21989. <https://doi.org/10.1080/19443994.2015.1125799>
21. Oliveira, F. S., et al. "Simple analytical method for determining electrical resistivity and sheet resistance using the van der Pauw procedure." *Scientific Reports* 10.1 (2020): 16379. <https://doi.org/10.1038/s41598-020-72097-1>
22. Krupka, Jerzy. "Contactless methods of conductivity and sheet resistance measurement for semiconductors, conductors and superconductors." *Measurement Science and Technology* 24.6 (2013): 062001 DOI [10.1088/0957-0233/24/6/062001](https://doi.org/10.1088/0957-0233/24/6/062001)
23. Náhlík, Josef, Irena Kašpárková, and Přemysl Fitl. "Study of quantitative influence of sample defects on measurements of resistivity of thin films using van der Pauw method." *Measurement* 44.10 (2011): 1968-1979. <https://doi.org/10.1016/j.measurement.2011.08.023>
24. Ramadan, Ahmed A., Robert D. Gould, and Ahmed Ashour. "On the Van der Pauw method of resistivity measurements." *Thin solid films* 239.2 (1994): 272-275. [https://doi.org/10.1016/0040-6090\(94\)90863-X](https://doi.org/10.1016/0040-6090(94)90863-X)
25. Jalal, Noor M., et al. "Effect of lithium chloride addition on the electrical conductivity of polyvinyl alcohol films." *American Journal of Engineering Research* 6.1 (2017): 337-343.pdf
26. Ellmer, Klaus. "Hall effect and conductivity measurements in semiconductor crystals and thin films." *Characterization of materials* (2012): 1-16.pdf
27. Cao, Shixiu, et al. "Hydrothermal synthesis of nanoparticles-assembled NiO microspheres and their sensing properties." *Physica E: low-dimensional systems and nanostructures* 118 (2020): 113655. <https://doi.org/10.1016/j.physe.2019.113655>
- 28 Bonomo, M. "Synthesis and characterization of NiO nanostructures: a review." *Journal of Nanoparticle Research* 20.8 (2018): 222. <https://doi.org/10.1007/s11051-018-4327-y>
- 29 .Song, Yuan-Jun, et al. "Investigation on the role of the molecular weight of polyvinyl pyrrolidone in the

- shape control of high-yield silver nanospheres and nanowires." *Nanoscale research letters* 9 (2014): 1-8. <https://doi.org/10.1186/1556-276X-9-17>
30. Mireles, Laura Karina, et al. "Physicochemical characterization of polyvinyl pyrrolidone: A tale of two polyvinyl pyrrolidones." *ACS omega* 5.47 (2020): 30461-30467. 168. Khan, A., et al. "Mechanistic study on methyl orange and congo red adsorption onto polyvinyl pyrrolidone modified magnesium oxide." *International Journal of Environmental Science and Technology* (2021): 1-14. <https://doi.org/10.1021/acsomega.0c04010>
31. Mohammed, Gh, Adel M. El Sayed, and W. M. Morsi. "Spectroscopic, thermal, and electrical properties of MgO/polyvinyl pyrrolidone/polyvinyl alcohol nanocomposites." *Journal of Physics and Chemistry of Solids* 115 (2018): 238-247. <https://doi.org/10.1016/j.jpics.2017.12.050>
32. Hashem, Manal, et al. "Fabrication and characterization of semiconductor nickel oxide (NiO) nanoparticles manufactured using a facile thermal treatment." *Results in physics* 6 (2016): 1024-1030. <https://doi.org/10.1016/j.rinp.2016.11.031>
33. Vani, G. Naga Sudha, et al. "Optical properties of PVP based polymer electrolyte films." *Int. J. Res. Eng. Adv. Technol.* 3 (2013): 7-12. <https://doi.org/10.1016/j.rinp.2016.11.031>
34. Baishya, Kaushik, and Karmakar Sanjib. "Study of Variation of Bandgaps of Pure and Doped Nickel Oxide Nanoparticles (NiO) prepared in different environments." *ABOUT IRJSE* (2017): 15. <https://oaji.net/articles/2017/731-1517243363.pdf>
35. Ali, Heba, Taha M. Tiama, and A. M. Ismail. "New and efficient NiO/chitosan/polyvinyl alcohol nanocomposites as antibacterial and dye adsorptive films." *International Journal of Biological Macromolecules* 186 (2021): 278-288. <https://doi.org/10.1016/j.ijbiomac.2021.07.055>
36. Al-Hada, Naif Mohammed, et al. "The impact of polyvinylpyrrolidone on properties of cadmium oxide semiconductor nanoparticles manufactured by heat treatment technique." *Polymers* 8.4 (2016): 113 . <https://doi.org/10.3390/polym8040113>.

الموصلية الكهربائية للأفلام الرقيقة المركبة من البولي فينيل بيروليديون مشوبة بجسيمات أكسيد النيكل النانوية

¹ زينب دخيل عبد علي ،² احمد عبد الاله احمد ،³ اسامة عبدالعزيز داخل،⁴ عمر الامين احمد ادم
[وزارة العلوم والتكنولوجيا، العراق، بغداد ،¹ وحدة ابحاث البوليمر ، كلية العلوم ، الجامعة المستنصرية، العراق
³ قسم الفيزياء ، كلية العلوم ، الجامعة المستنصرية، العراق
⁴ قسم الكيمياء ، كلية العلوم والفنون في الجوراشي ، جامعة الباحة ، الباحة ، المملكة العربية السعودية
zainabdakheel@uomustansiriyah.edu.iq

الخلاصة:

تم تحضير اغشية من بوليمر بولي فاينيل بيروليديون مشوبة بنسب وزنية مختلفة من جسيمات اوكسيد النيكل النانوي (0.02-0.2%) التي انتجت باستخدام الطريقة الحرارية المائية ذات الدرجات الحرارية المنخفضة. باستخدام تحليل حيود الاشعة السينية و تحليل فورييه للاشعة تحت الحمراء تم فحص التركيب البلوري للجسيمات النانوية. تم التحقق من مورفولوجية الاغشية المشوبة باستخدام فحص المجهر الالكتروني الماسح و مجهر القوة الذرية، تم تمييز الخصائص البصرية للفيلم الرقيق المركب. اظهر نمط حيود الاشعة السينية ان اوكسيد النيكل له تركيب بلوري متعدد مكعب. اجريت قياسات تحويل فورييه للطيف بالاشعة تحت الحمراء لبوليمر بولي فاينيل بيروليديون المشوب باكاسيد المعدن النانوية ، حيث اظهر اختلاف واضح عن البوليمر النقي حيث ظهرت رابطة Ni-O عند الطول الموجي 408 سم⁻¹. لتأكيد تأثير إضافة NiO على الترابط الكيميائي لأفلام بولي فاينيل بيروليديون تم استخدام قياسات معامل هول لحساب الخصائص الكهربائية بما في ذلك التوصيلية حركية ناقلات الشحنة ونوعها. اظهرت نتائج قياسات معامل هول بان افضل توصيلية تم الحصول عليها عند النسبة الوزنية (0.2%) لاوكسيد النيكل النانوي تساوي (2*10⁻⁴ سيمنز) حيث تم تحضير غشاء شبة موصل يمكن استخدامه في المتحسسات وتطبيقات الخلايا الشمسية.

الكلمات المفتاحية: بوليمر بولي فاينيل بيروليديون، جسيمات نانوية من اوكسيد النيكل، التوليف الحراري المائي، التوصيل الكهربائي، فيلم رقيق مركب، بوليمر موصل.